Simultaneous activation of NADPH oxidase-related proton and electron currents in human neutrophils

T. E. DeCoursey*†, V. V. Cherny*, W. Zhou*, and L. L. Thomas‡

Departments of *Molecular Biophysics and Physiology and ‡Immunology/Microbiology, Rush Presbyterian St. Luke's Medical Center, Chicago, IL 60612

Edited by Charles F. Stevens, The Salk Institute for Biological Studies, La Jolla, CA, and approved March 28, 2000 (received for review February 2, 2000)

Generation of reactive oxygen species by the NADPH oxidase complex is an important bactericidal weapon of phagocytes. Phorbol myristate acetate (PMA) is a potent agonist for this "respiratory burst" in human neutrophils. Although stoichiometric H^+ efflux occurs during the respiratory burst, efforts to stimulate voltage-gated H^+ channels by PMA in whole-cell patch-clamped phagocytes have been unsuccessful. We have used a modification of the permeabilized-patch configuration that allows control of intracellular pH and preserves second-messenger pathways. Using this method, we show that PMA dramatically enhances and alters voltage-gated proton currents in human neutrophils. PMA produced four alterations in H^+ current properties, each of which increases the H^+ current at any given voltage: (*i*) a 40-mV negative shift in the H^+ conductance-voltage (g_H–V) relationship; (*ii*) faster activation [smaller activation time constant (τ_{act})] during depolarizing pulses; (*iii*) slower deactivation [larger deactivation time constant (τ_{tail})] on repolarization; and (*iv*) a larger maximum H^+ conductance ($g_{H,max}$). Inward current that directly reflects electron transport by NADPH oxidase was also activated by PMA stimulation. The identity of this electron current was confirmed by its sensitivity to diphenylene iodinium, an inhibitor of NADPH oxidase. Diphenylene iodinium also reversed the slowing of τ_{tail} with a time course paralleling the inhibition of electron current. However, the amplitudes of H^+ and electron currents activated by PMA were not correlated. A complex interaction between NADPH oxidase and voltage-gated proton channels is indicated. The data suggest that PMA stimulation modulates preexisting H^+ channels rather than inducing a new H^+ channel.

respiratory burst | hydrogen ion | pH | proton channel | ion channels

NADPH oxidase is a major bactericidal weapon of neutrophils and other phagocytes (1). On stimulation, the enzyme complex assembles in the membrane and produces superoxide anion, the precursor to several bactericidal reactive oxygen species. NADPH oxidase is electrogenic (2), releasing a proton into the cytoplasm for each superoxide anion released into the phagocytic vacuole or extracellular medium. As a result, pH changes reflecting increased H^+ permeability are seen during the respiratory burst in phagocytes (2, 3) after stimulation by the phorbol ester, phorbol 12-myristate 13-acetate (PMA). Voltage-gated proton channels, discovered in snail neurons (4), were postulated to mediate the increased H^+ permeability during the respiratory burst in human neutrophils (2, 5, 6). The importance of H^+ efflux as a means of charge compensation is emphasized by the inhibition of PMA-stimulated superoxide anion production by Zn^{2+} or Cd^{2+}, which presumably act by inhibiting proton current (7, 8). However, attempts to demonstrate effects of PMA on H^+ currents in phagocytes studied in the whole-cell patch-clamp configuration have heretofore been unsuccessful. It is therefore unclear whether the g_H observed in phagocytes by conventional recording is the same conductance that is activated during the respiratory burst in intact cells. Furthermore, a recent report described a distinct "novel" variety of voltage-gated proton current in human eosinophils studied in whole-cell configuration under conditions that activated NADPH oxidase (9). We have undertaken this study in part to resolve the identity of the proton channels that are activated during the respiratory burst in human neutrophils. To accomplish this, we have developed a variant of the permeabilized-patch technique (10–13) that permits a vigorous response to PMA. The ability to observe H^+ current enhancement and NADPH oxidase-mediated electron flux simultaneously permits dissection of the relationships between these processes.

Methods

Neutrophils were isolated from the blood of healthy adult donors, under informed consent, by density gradient centrifugation (14) and kept on ice before use. Type II alveolar epithelial cells were isolated from adult male Sprague–Dawley rats by using enzyme digestion, lectin agglutination, and differential adherence, and maintained in primary tissue culture, as described elsewhere (15). Standard patch-clamp techniques at 20°C, with modifications described below, and computerized data acquisition and analysis were used (15). For whole-cell recording, the bath and pipette solutions contained 100 mM buffer near its pK_a, tetramethylammonium methanesulfonate to bring the osmolarity to ≈300 mOsm, 1 mM EGTA, and 2 mM $MgCl_2$ or $CaCl_2$ (Sigma). For permeabilized patch recording, the pipette and bath solutions usually contained 50 mM NH_4^+ in the form of 25 mM $(NH_4)_2SO_4$ (Aldrich), 2 mM $MgCl_2$, 5 mM BES buffer, and 1 mM EGTA, and were titrated to pH 7.0 with tetramethylammonium hydroxide. We added ≈500 μg/ml solubilized amphotericin B (≈45% purity) (Sigma) to the pipette solution, after first dipping the tip in amphotericin-free solution.

Results

As illustrated in Fig. 1*A*, exposure of a human neutrophil in the whole-cell configuration to 60 nM PMA for >20 min had no discernable effect on the amplitude or gating kinetics of voltage-gated H^+ currents. One possible explanation for the failure of PMA to act in this configuration is the disruption of intracellular signaling pathways by dialysis with the pipette solution. In this study, we have used the "permeabilized patch" configuration (10, 11) to preserve the cytoplasmic contents. For this, we added the pore-forming antibiotic amphotericin B to the pipette solution (12). Amphotericin partitions into the patch of membrane spanning the pipette tip and allows small ions (hence electrical current) to pass between the pipette and the cytoplasm. This technique cannot be used to study proton currents, because high concentrations of buffer are required in the cell to control

This paper was submitted directly (Track II) to the PNAS office.

Abbreviations: DPI, diphenylene iodinium; E_H, Nernst potential for H^+; I_e, electron current; I_H, H^+ current amplitude; g_H, H^+ chord conductance; $g_{H,max}$, maximum H^+ chord conductance; pH_o, extracellular pH; pH_i, intracellular pH; PMA, phorbol 12-myristate 13-acetate; τ_{act}, activation time constant; τ_{tail}, tail current (deactivation) time constant; V_{hold}, holding potential; V_{rev}, reversal potential.

†To whom reprint requests should be addressed. E-mail: tdecours@rush.edu.

The publication costs of this article were defrayed in part by page charge payment. This article must therefore be hereby marked "*advertisement*" in accordance with 18 U.S.C. §1734 solely to indicate this fact.

Article published online before print: *Proc. Natl. Acad. Sci. USA*, 10.1073/pnas.100047297. Article and publication date are at www.pnas.org/cgi/doi/10.1073/pnas.100047297

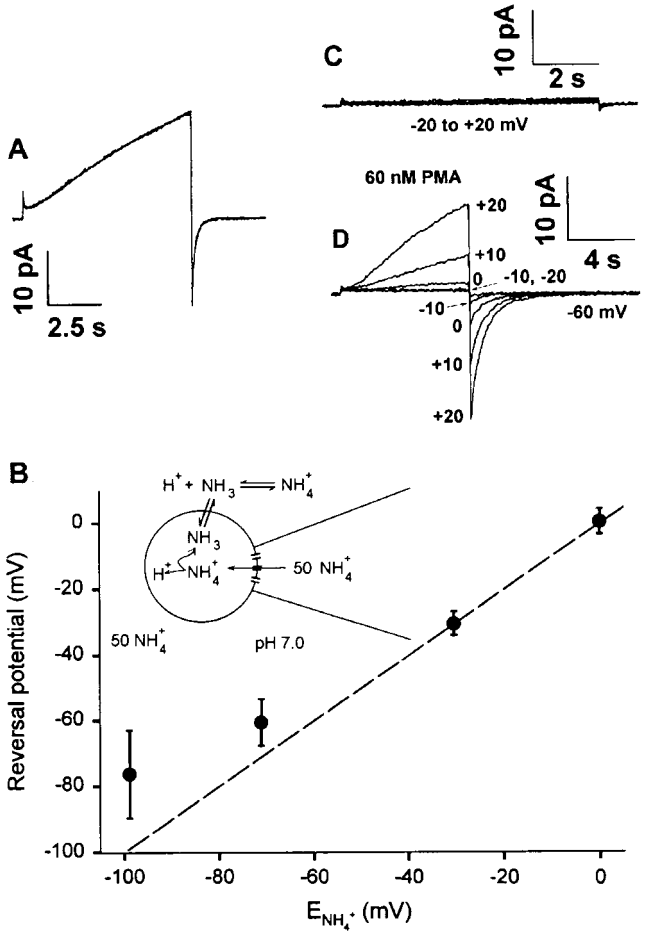

Fig. 1. PMA has no effect on human neutrophils in conventional whole-cell configuration but produces dramatic effects in permeabilized patches. (*A*) Lack of effect of PMA in a human neutrophil studied in conventional whole-cell recording configuration. After 16 min in whole-cell configuration, 60 nM PMA was applied. Superimposed are currents during test pulses to +60 mV applied from a holding potential (V_{hold}) of −40 mV just before PMA was added and 23 min later. The bath and pipette solutions were identical to those used to study PMA effects in permeabilized-patch recordings (see *Methods*). (*B*) Creating an NH_4^+ gradient has been shown to establish pH_i in whole-cell configuration (13, 17). To validate this approach for amphotericin-permeabilized patch recording, we determined the reversal potential, V_{rev}, of H^+ currents in human neutrophils. Average V_{rev} data are plotted against the Nernst potential for NH_4^+, E_{NH4}^+, which ideally is the same as E_H if the NH_4^+ gradient successfully establishes pH_i. Mean ±SD values of V_{rev} are plotted for 5, 12, 15, and 51 neutrophils (*Left* to *Right*) in 1-, 3-, 15-, and 50-mM NH_4^+ bath solutions, respectively. These data confirm that NH_4^+ can permeate amphotericin pores, because otherwise pH_i would be uncontrolled, and V_{rev} would have been the same in all solutions. The dashed line shows the Nernst potential for NH_4^+ that would obtain if the NH_4^+ gradient controlled pH_i perfectly and if the H^+ channel were perfectly selective for H^+, which appears the case (18). The control of pH_i is excellent with gradients ≤10. Because we are interested in physiological responses, we operated in the range of a 50//50 or 15//50 gradient ($pH_i = pH_o$ or $pH_i = pH_o - 0.5$), where the control is excellent. V_{rev} was similar before and after PMA treatment, with an average change of <4 mV in 12 cells where V_{rev} was measured in the same solutions before and after PMA. When the permeabilized-patch configuration is used, PMA has dramatic effects on H^+ currents. Identical families of voltage pulses were applied to a human neutrophil before (*C*) and after (*D*) 10-min exposure to 60 nM PMA. From a holding potential of −60 mV, 8-s pulses were applied to −20 mV through +20 mV in 10-mV increments. The inward tail currents after repolarization to −60 mV are labeled with the test pulse voltage. The presence of a distinct inward tail current after the pulse to −10 mV reveals activation of the H^+ conductance negative to the tail current reversal potential, V_{rev}, measured in this cell, −3 mV. Before PMA was added, depolarizing pulses larger than shown in *C* elicited "normal" H^+ currents.

intracellular pH (pH_i) (16), and buffer molecules are too large to pass through amphotericin pores. To overcome this limitation, we created an NH_4^+ gradient (Fig. 1*B Inset*), made possible because NH_4^+ does permeate amphotericin pores. Fig. 1*B* shows that the reversal potential of H^+ currents (V_{rev}) reflects the pH gradient predicted on the assumption that the applied NH_4^+ gradient sets pH_i (13, 17). Control over pH_i effected by varying extracellular [NH_4^+] at constant internal [NH_4^+] is excellent except for large NH_4^+ gradients. Therefore we used a zero gradient in most experiments, with 50 mM NH_4^+ in the bath and in the pipette, setting extracellular pH (pH_o) = pH_i = 7.0.

PMA dramatically enhanced H^+ currents in neutrophils studied in the permeabilized patch configuration. Voltage-gated proton currents in unstimulated neutrophils, as in other cells, are activated only positive to the Nernst potential for protons (E_H) (6, 18). With a symmetrical pH gradient (pH_o = pH_i = 7.0), threshold is ≥+20 mV, and a pulse to +20 mV elicited only tiny current (Fig. 1*C*). However, the same voltage pulses elicited large H^+ currents 10 min after addition of 60 nM PMA to the bath (Fig. 1*D*). The activation of H^+ currents by PMA in human neutrophils evidently requires a cytoplasmic component that is inactivated or dialyzed away in conventional whole-cell configuration.

During permeabilized patch recording, stimulation by PMA consistently produced four effects on H^+ currents in human neutrophils, each of which promotes H^+ efflux: (*i*) faster activation; (*ii*) slower deactivation; (*iii*) a larger maximum g_H ($g_{H,max}$); and (*iv*) a 40-mV negative shift of the voltage-activation curve. Before PMA ("pre," Fig. 2*A*), a pulse to +60 mV elicited a slowly activating outward H^+ current. On repolarization to −40 mV, the inward tail current reflects the time course of H^+ channel closing. Shortly after 60 nM PMA was added to the bathing solution, the H^+ current amplitude (I_H) began to increase, more than doubling within 10 min (●, Fig. 2*B*). On average, I_H increased by a factor of 3.3 (Table 1). The H^+ current turned on with depolarization more rapidly after PMA. Fitted by a single exponential after a delay, the activation time constant (τ_{act}) decreased to 27% of its initial value (Table 1). The third effect of PMA was to slow the decay of H^+ tail currents. This slowing was progressive (Fig. 2*A*) and occurred at the same time the outward current was increasing. The tail currents at all times could be fitted by a single exponential (curves superimposed on the data points). This result suggests that the properties of H^+ channels change in a graded manner, rather than in an all-or-none fashion. In some cells, however, we observed more complex kinetics. On average, the tail current (deactivation) time constant (τ_{tail}) at −40 mV was slowed by a factor of 5.5 (Table 1).

Inspection of Fig. 2*A* reveals a small increase in the inward holding current at −40 mV after PMA was added. This additional current reflects the activity of the NADPH oxidase, which transports electrons out of the cell. This electron efflux is directly measurable as an inward membrane current (19). We confirmed the identity of the electron current (I_e) by using diphenylene iodinium (DPI), an inhibitor of NADPH oxidase function (20). The appearance of I_e demonstrates that the NADPH oxidase was activated under the conditions used. The average amplitude of I_e was −2.3 pA (Table 1), which is several times smaller than −15.6 pA (19) or −7.5 pA (9) measured in human eosinophils. This result is consistent with the 5-fold higher rate of superoxide anion release by human eosinophils when stimulated with PMA as compared with human neutrophils (21). DPI (at 1 or 10 μM) abolished I_e activated by PMA but did not inhibit the NADPH oxidase-associated H^+ current (Fig. 2 *B* and *C*). The faster activation of I_H (▲, Fig. 2*B*) and the leftward shift of the g_H–V relationship also were unaffected by DPI (data not shown). Thus I_H remains enhanced even after abolition of NADPH oxidase function (detected as I_e). The dramatic slowing of tail current decay, however, was largely reversed by DPI (Fig. 2*C*).

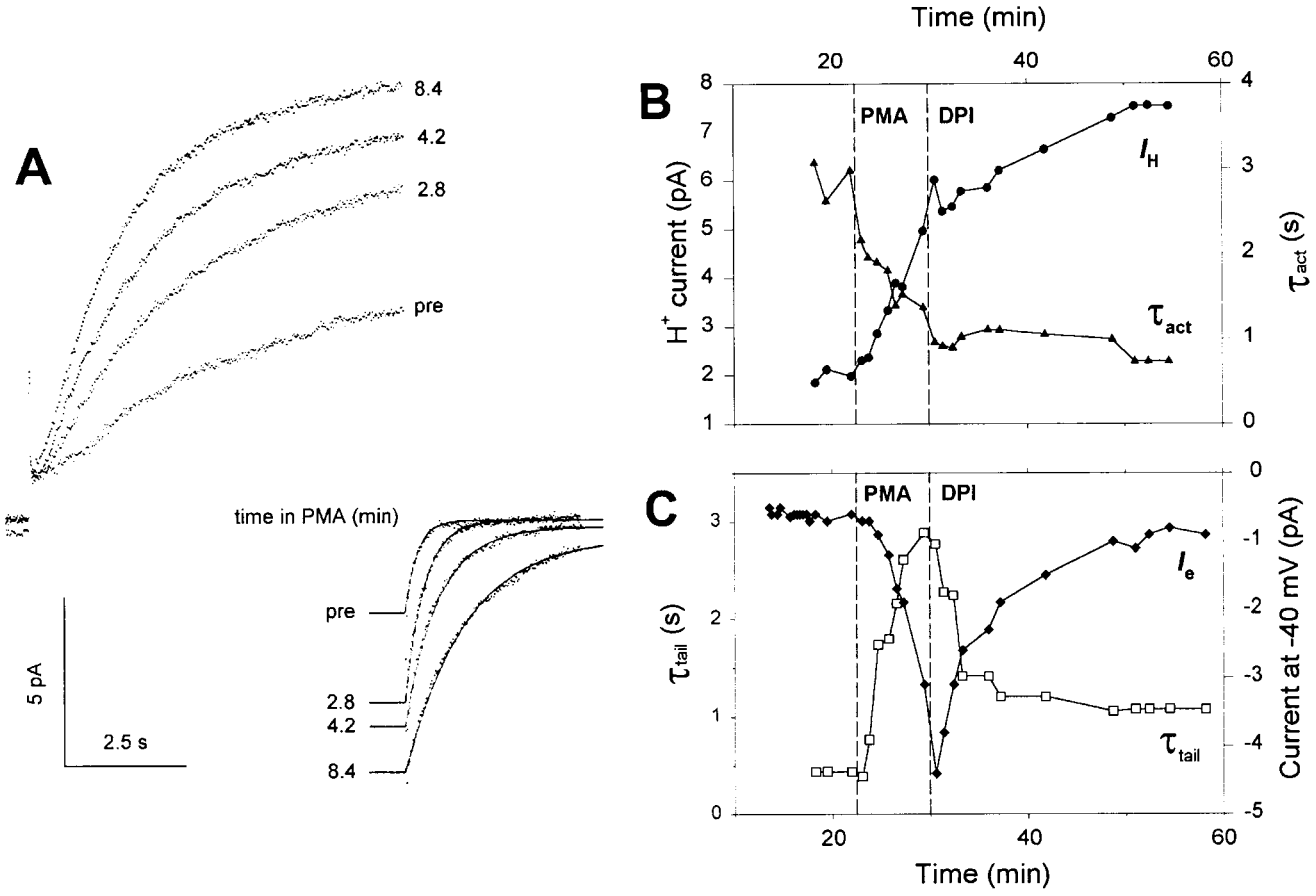

Fig. 2. Time course of effects of PMA on H^+ currents and electron currents. (*A*) Progressive enhancement of H^+ currents by PMA. Test pulses were applied to +60 mV from $V_{hold} = -40$ mV in amphotericin-permeabilized patch configuration in a human neutrophil. I_H during a control pulse is shown (''pre'') and during three identical pulses after 60 nM PMA. I_H increased progressively, as did the initial amplitude of the tail currents (on return to −40 mV). The tail currents are fitted by single exponentials (continuous lines) with amplitude and time constants (−2.8 pA, 260 ms; −5.5 pA 410 ms; −5.9 pA, 700 ms; and −7.0 pA, 1270 ms, respectively, in chronological order). Although single exponential fits were not perfect, the data could not be fitted by simply varying the relative amplitudes of fixed fast and slow components. The holding current did not change until the last pulse shown in PMA, when there was a net −0.5 pA inward current (relative to the holding current before PMA). This inward current reflects electron current arising from NADPH oxidase action (19). (*B* and *C*) Time course of the changes in H^+ and inward electron current, I_e, in a neutrophil exposed to 60 nM PMA and then to 1 μM DPI. (*B*) After PMA was added (dashed vertical line), I_H (●) increased progressively, and activation became faster (the activation time constant, τ_{act}, (▲) decreased). Both I_H and τ_{act} were obtained by fitting the rising current with a single exponential after a delay. Neither effect was reversed by DPI (second dashed vertical line). The −40 mV shift of the g_H–V relationship similarly was not reversed by DPI (not shown). (*C*) In the same cell, PMA greatly slowed τ_{tail} (□) and activated an inward current at −40 mV (right axis) that increased with a similar time course (◆). The NADPH oxidase inhibitor, DPI eliminated the additional inward I_e and largely reversed the slowing of τ_{tail} with a similar time course.

The time courses of PMA effects are compared in Fig. 2 and Table 1. The increase in the rate of channel opening was the fastest response (▲, Fig. 2*B*), with a half-time <1 min in most cells. Because τ_{act} decreased substantially before I_e turned on, this change cannot be a consequence of oxidase function. In contrast, the increase in I_H (●) and the slowing of τ_{tail} (□) occurred more slowly, with time courses similar to that of the activation of I_e (◆). Intriguingly, DPI reversed the slowing of τ_{tail} over several minutes, paralleling the time course of its inhibition of I_e (Fig. 2*C*). If DPI had a direct pharmacological effect on H^+ channels, one would expect a rapid change; furthermore, DPI did not change τ_{tail} in unstimulated neutrophils or alveolar epithelial cells (data not shown). The similar time courses of changes in I_e and τ_{tail} suggest an intimate or causal relationship between the function of NADPH oxidase and this aspect of H^+ channel behavior. DPI interferes directly with the function of NADPH oxidase rather than preventing its activation or removing its products (20) and thus acts by a mechanism distinct from

Table 1. Magnitude and time course of effects of PMA

	τ_{act}	τ_{tail}	I_H	I_e, pA
PMA/control	0.27 ± 0.05 (14)	5.5 ± 1.3 (11)	3.3 ± 1.9 (11)	−2.3 ± 1.5 (15)
Half-time, min	<1	4.3 ± 3.2 (11)	3.4 ± 2.4 (10)	3.0 ± 1.63 (11)

The average ratio of each parameter measured after treatment with 60 nM PMA to its value before treatment. Usually, I_H and τ_{act} were measured during pulses to +60 mV and τ_{tail} and I_e at −40 mV. I_e is taken as the average increase in inward current after PMA. Mean ±SD is given for (*n*) observations.

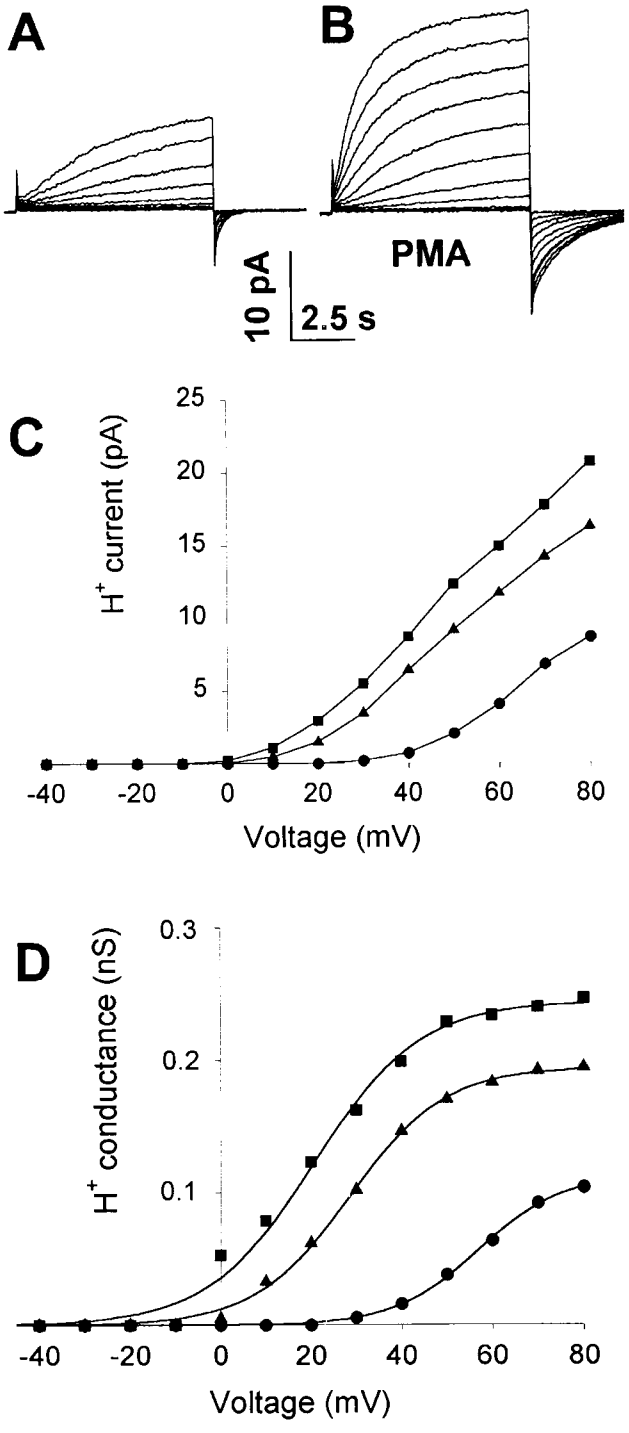

Fig. 3. PMA shifts the g_H-V relationship to voltages 40 mV more negative. Families of voltage-clamp currents are shown in a human neutrophil in permeabilized-patch configuration before (*A*) and 21 min after (*B*) addition of 60 nM PMA to the bath. In both *A* and *B*, the holding potential, V_{hold}, was −40 mV, and test pulses are shown from −20 mV to +80 mV in 10-mV increments. The holding current is offset by about −0.5 pA in *B* relative to *A* because of putative electron current. (*C*) H^+ current—voltage relationships for the control run from *A* (●), a family recorded starting 6 min after addition of PMA (▲), and the family shown in *B* (■), (*D*) Chord conductance—voltage relationships for the three families in (*C*), with identical symbol meanings. Curves show the best-fitting simple Boltzmann functions, with midpoint voltage, slope factor, and fitted $g_{H,max}$, respectively, 57 mV, 9.3 mV, and 0.11 nS (●); 29 mV, 10.6 mV, and 0.19 nS (▲); and 21 mV, 11.8 mV, and 0.24 nS (■).

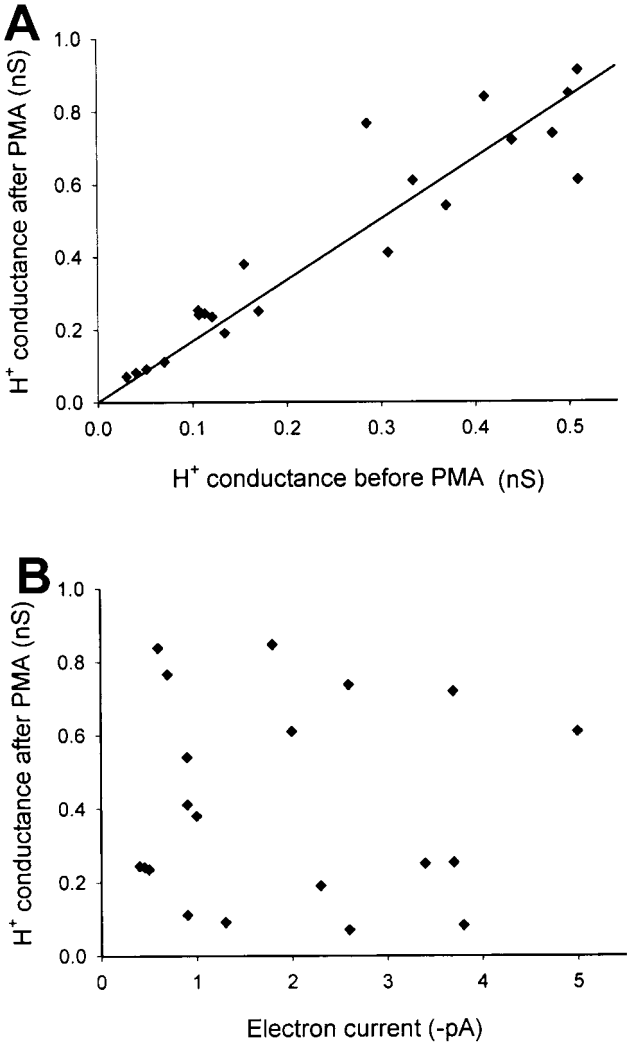

Fig. 4. The limiting $g_{H,max}$ in individual neutrophils after stimulation with PMA is correlated with the resting H^+ conductance but not with the electron current. (*A*) The maximum H^+ conductance, $g_{H,max}$, was estimated from the upper limit of Boltzmann fits of the g_H–V relationships, like those in Fig. 3. The linear regression line (constrained to pass through the origin) indicates an average ≈1.7-fold enhancement of $g_{H,max}$ after PMA. This increase is less than the average increase in I_H in Table 1, because the latter measurement was at a fixed voltage that in unstimulated neutrophils does not elicit maximal activation. (*B*) In contrast, there was no correlation between $g_{H,max}$ and electron current amplitude (measured at −40 mV) in neutrophils after stimulation with PMA. Similarly, there was no correlation between I_e and the PMA-stimulated fraction of the g_H (data not shown).

the signaling cascade through which PMA activates the oxidase. The mechanism by which DPI reverses the effects of PMA of τ_{tail} thus appears to involve the activity of the oxidase itself.

Fig. 3 illustrates families of H^+ currents in a neutrophil before (*a*) and 21 min after (*b*) stimulation with PMA. The corresponding current–voltage relationships are plotted in Fig. 3*C* (●, ■), including an intervening family recorded 6 min after PMA stimulation (▲). The current amplitude, I_H, was determined by fitting the current at each voltage with an exponential after a delay. Corresponding conductance–voltage relationships are plotted in Fig. 3*D*. Fitted by a Boltzmann function after the PMA effects appeared to reach steady state (>10 min), the midpoint voltage was shifted on average −38.8 ± 11.8 mV (mean ± SD) in 20 neutrophils. The slope factors mostly ranged 7–12 mV and

did not change consistently. The limiting g_H, $g_{H,max}$ increased on average 1.9 ± 0.4 times (n = 21). If PMA activated a new variety of H^+ channel without affecting preexisting channels, one would expect superposition of two Boltzmann distributions. Instead, the g_H–V relationship appeared to shift progressively, with no indication of multiple components. Although indirect, the evidence points to modification of preexisting channels rather than simple superposition of new channels on preexisting ones.

Further, if PMA stimulation turned on a novel H^+ conductance that is independent of the H^+ conductance in unstimulated neutrophils, there is no *a priori* reason to expect a correlation between their amplitudes. As shown in Fig. 4*A*, the total H^+ conductance after PMA stimulation was linearly related to the H^+ conductance in each cell before stimulation. In contrast, there was no correlation between the amplitudes of H^+ currents and electron currents, when compared in individual cells (Fig. 4*B*). The latter result is not easy to reconcile with the idea that the H^+ channel activated during the respiratory burst is a part of the NADPH oxidase complex (22, 23).

To determine whether the PMA effect on H^+ currents is unique to phagocytes, rat alveolar epithelial cells in permeabilized patch configuration with an NH_4^+ gradient were exposed to PMA. Rat alveolar epithelial cells express a high density of voltage-gated proton channels (18, 24, 25), with properties different from those in neutrophils. No consistent change in either the H^+ current amplitude or in gating kinetics was detected in six epithelial cells studied for up to 45 min after PMA treatment (data not shown). The PMA response in neutrophils may be specific to phagocyte H^+ channels or may require factors that are present in phagocytes but not in epithelial cells.

Discussion

Recent studies indicate that most NADPH oxidase activity in PMA-stimulated human neutrophils is detected in secretory granules that subsequently fuse with the plasma membrane (26). Thus, ''activation'' of NADPH oxidase occurs to some extent when secretory vesicles that contain its components fuse with the plasma membrane. Similarly, some of the enhancement of the H^+ conductance may result from insertion of H^+ channels stored in the same secretory vesicle membranes. Consistent with this idea, the stimulation of superoxide anion production by NADPH oxidase (detected directly as electron current) has a similar time course as I_H enhancement. That the enhanced I_H after PMA is not reversed by DPI suggests that the channels remain in the plasma membrane independently of oxidase function. The slowing of τ_{tail} by PMA was reversed by DPI, as though NADPH oxidase activity in itself modifies this H^+ channel property. For example, protons released intracellularly may lower the local pH near H^+ channels, stabilizing the open state (25).

The properties of H^+ currents observed after stimulation with PMA resemble those of a ''novel'' proton conductance reported in human eosinophils under conditions supporting NADPH oxidase activity (9). Compared with ''ordinary'' proton channels, novel H^+ channels exhibit slower tail current decay and activate at more negative voltages, thus uniquely permitting inward H^+ current (9). In PMA-treated neutrophils, H^+ tail currents decayed 5.5 times more slowly (Table 1), and inward currents were detected at voltages just negative to E_H (Fig. 1*D*), because the voltage-activation curve was shifted so that threshold was negative to E_H (Fig. 3*D*). The properties of PMA-altered H^+ currents resolve a puzzling discrepancy. In whole-cell experiments in human neutrophils, voltage-gated proton channels do not conduct steady-state inward current (6, 18), yet both outward and inward PMA-activated H^+ fluxes have been observed in neutrophils (5, 27, 28). The novel H^+ currents were proposed to coexist with normal H^+ channels in phagocytes (9). Considered together, however, the progressive changes in H^+ current properties, the correlation between the H^+ conductances before and after PMA stimulation, and the fact that DPI reversed the slowing of τ_{tail} without reducing $g_{H,max}$, are most simply explained if PMA alters the properties of ''normal'' H^+ channels, rather than introducing a new type.

We appreciate helpful discussions about permeabilized patch recording with Dick Horn, Stephen Korn, and Jim Rae. This work was supported in part by National Institutes of Health Grants HL52671 to T.D. and AI32041 to L.T.

1. Babior, B. M. (1999) *Blood* **93,** 1464–1476.
2. Henderson, L. M., Chappell, J. B. & Jones, O. T. (1987) *Biochem. J.* **246,** 325–329.
3. Kapus, A., Szászi, K. & Ligeti, E. (1992) *Biochem. J.* **281,** 697–701.
4. Thomas, R. C. & Meech, R. W. (1982) *Nature (London)* **299,** 826–828.
5. Nanda, A. & Grinstein, S. (1991) *Proc. Natl. Acad. Sci. USA* **88,** 10816–10820.
6. DeCoursey, T. E. & Cherny, V. V. (1993) *Biophys. J.* **65,** 1590–1598.
7. Henderson, L. M., Chappell, J. B. & Jones, O. T. (1988) *Biochem. J.* **255,** 285–290.
8. Lowenthal, A. & Levy, R. (1999) *J. Biol. Chem.* **274,** 21603–21608.
9. Bánfi, B., Schrenzel, J., Nüsse, O., Lew, D. P., Ligeti, E., Krause, K. H. & Demaurex, N. (1999) *J. Exp. Med.* **190,** 183–194.
10. Lindau, M. & Fernandez, J. M. (1986) *Nature (London)* **319,** 150–153.
11. Horn, R. & Marty, A. (1988) *J. Gen. Physiol.* **92,** 145–159.
12. Rae, J., Cooper, K., Gates, P. & Watsky, M. (1991) *J. Neurosci. Methods* **37,** 15–26.
13. Grinstein, S., Romanek, R. & Rotstein, O. D. (1994) *Am. J. Physiol.* **267,** C1152–C1159.
14. Haskell, M. D., Moy, J. N., Gleich, G. J. & Thomas, L. L. (1995) *Blood* **86,** 4627–4637.
15. Cherny, V. V. & DeCoursey, T. E. (1999) *J. Gen. Physiol.* **114,** 819–838.
16. DeCoursey, T. E. & Cherny, V. V. (1996) *Biophys. J.* **71,** 182–193.
17. DeCoursey, T. E. & Cherny, V. V. (1997) *J. Gen. Physiol.* **109,** 415–434.
18. DeCoursey, T. E. & Cherny, V. V. (1994) *J. Membr. Biol.* **141,** 203–223.
19. Schrenzel, J., Serrander, L., Bánfi, B., Nüsse, O., Fouyouzi, R., Lew, D. P., Demaurex, N. & Krause, K. H. (1998) *Nature (London)* **392,** 734–737.
20. Robertson, A. K., Cross, A. R., Jones, O. T. & Andrew, P. W. (1990) *J. Immunol. Methods* **133,** 175–179.
21. Yagisawa, M., Yuo, A., Yonemaru, M., Imajoh-Ohmi, S., Kanegasaki, S., Yazaki, Y. & Takaku, F. (1996) *Biochem. Biophys. Res. Commun.* **228,** 510–516.
22. Henderson, L. M., Banting, G. & Chappell, J. B. (1995) *J. Biol. Chem.* **270,** 5909–5916.
23. Henderson, L. M. & Meech, R. W. (1999) *J. Gen. Physiol.* **114,** 771–786.
24. DeCoursey, T. E. (1991) *Biophys. J.* **60,** 1243–1253.
25. Cherny, V. V., Markin, V. S. & DeCoursey, T. E. (1995) *J. Gen. Physiol.* **105,** 861–896.
26. Kobayashi, T., Robinson, J. M. & Seguchi, H. (1998) *J. Cell Sci.* **111,** 81–91.
27. Henderson, L. M. & Chappell, J. B. (1992) *Biochem. J.* **283,** 171–175.
28. Nanda, A. & Grinstein, S. (1995) *J. Cell. Physiol.* **165,** 588–599.